

Biodegradation of *Phormium tenax*/Poly(lactic acid) Composites

E. Fortunati,¹ D. Puglia,¹ C. Santulli,² F. Sarasini,² J. M. Kenny¹

¹University of Perugia, UdR INSTM, Department of Civil and Environmental Engineering, Strada di Pentima 4, 05100 Terni, Italy

²Department of Chemical Engineering Materials Environment, Sapienza Università di Roma, Via Eudossiana 18, 00184 Roma, Italy

Received 26 June 2011; accepted 13 January 2012

DOI 10.1002/app.36839

Published online in Wiley Online Library (wileyonlinelibrary.com).

ABSTRACT: The disintegration patterns of composites produced by a melt compounding process using 0, 20, 30, and 40 wt % of *Phormium tenax* fibers in poly(lactic acid) (PLA) matrix were studied for a period of 40 days in composting conditions. The characterization of PLA and PLA/*phormium* composites included disintegration measurements, differential scanning calorimetry, FTIR analysis, thermogravimetric analysis, and scanning electron microscopy. The two controlling factors for disintegrability appeared to be the crystallinity of PLA and *phormium*

fiber content: in general, the matrix tends to disintegrate completely before the 40 days and also *phormium* fibers undergo a substantial degradation during this period of time. Measurements taken at 10, 20, 30, and 40 days confirm that the disintegration process progresses steadily, though most of it takes place between 20 and 30 days. © 2012 Wiley Periodicals, Inc. *J Appl Polym Sci* 000: 000–000, 2012

Key words: biodegradable; biofibers; biopolymers; thermal properties

INTRODUCTION

The introduction of plant fibers as reinforcement in biodegradable polymer matrices may contribute to improving their mechanical properties, making them more suitable to the use in semistructural components, for example, as electronic products.¹ Nowadays, as a result of growing environmental awareness, biodegradation of the obtained composite has a particular significance, since a sustainable end-of-life scenario is required for the material. The degradation of properties of the plant fiber composite should ideally be controllable in the whole range of reinforcement volumes applied, so that the modification of the decomposition patterns with respect to the pure polymer is known.²

Poly(lactic acid) (PLA) is prepared from renewable agricultural raw materials fermented to lactic acid, then polymerized, tailoring the molecular weights distribution according to the requirements: in particular, the proportion of the L- and D- isomeric forms will determine the properties of the polymer, i.e., whether the material is amorphous or semicrystalline.^{3,4} As far as biodegradability is concerned, previous studies confirm that PLA is naturally

degraded in soil or compost,⁵ although it is less susceptible to degradation in natural environment than other aliphatic biodegradable polymers, such as poly(3-caprolactone) (PCL).⁶ This is in favor of its use with plant fibers as reinforcement, so that a fully biodegradable and hopefully compostable material is obtained.⁷

The polymer erodes mainly by hydrolysis: the attack of water molecules lead to its random decomposition into oligomers.⁸ The final degradation product, lactic acid, is a metabolic product of all animals and microorganisms, deemed to be nontoxic, which can be easily disposed of by composting or land filling.⁹ It is essential that this characteristic is retained in the plant fiber composite obtained, a result which of course strongly depends on the species from which the fiber is extracted and on fiber morphology.

In particular, New Zealand Flax is a monocotyledon indigenous to New Zealand and Norfolk Island, until recently attributed to the Agavaceae family, now more frequently referred to as belonging to the Hemerocallidaceae.¹⁰ Two species of the genus *Phormium* are native to New Zealand: *Phormium tenax* (also known as harakeke) and *Phormium cookianum* (also known as wharariki), the key difference being the way their seed pods grow. *Phormium* represented an important resource in Maori life. The traditional use of *phormium* leaves in the Maori culture was making plaiting mats and containers, whereas extracted fibers have been used for fishing nets, ropes, baskets, and cloaks.¹¹ During last years,

Correspondence to: C. Santulli (carlo.santulli@uniroma1.it).

several articles appeared concerning the use of *Phormium tenax* fibers as potential reinforcement in both thermoplastic and thermosetting matrices.^{12–15}

Most recently a work was performed on their introduction also in PLA matrix, which demonstrated that the use of phormium fiber content of up to 40 wt % is suitable for polymer reinforcement.¹⁵ In particular, a full account of the mechanical properties of PLA-phormium composites, including data for the matrix alone, was given there, where a substantial increase of composite stiffness, but no improvement of tensile properties was obtained by fiber addition. This was attributed to the poor adhesion between phormium fibers and to the consequent not very effective stress transfer across the interphase.¹⁵ The large quantity of fiber used in Ref. 15 posed the problem of how much the degradation patterns of PLA are modified with growing phormium fiber content, which is the objective of this study.

In this research, melt compounding extrusion process was explored as a technique of preparing phormium fiber-based composites. PLA composites were produced using different content of natural fibers and the thermal stability of the new systems, their morphology and chemical properties were extensively investigated. Moreover, the disintegrability in composting conditions of PLA composites was studied to gain insights into the post-use degradation processes.

EXPERIMENTAL METHODS

Materials

PLA 3051D, with a specific gravity of 1.25 g/cm³, a melt flow index (MFI) of 7.75 g/10 min (210°C, 2.16 kg) and a nominal melting temperature of 170°C, was supplied by Nature Works®, USA. PLA resin 3051D had 96% L-Lactide to 4% D-Lactide units.¹⁶

Phormium tenax fibers were collected from Templeton Mill, Riverton, New Zealand. Leaves were stripped and the hanks of fibers were washed and then paddocked and scutched, according to the typical procedure followed on these fibers.¹⁷ As from properties reported for all gauge lengths in Ref. 18, the average diameter of the fibers was equal to 164.8 ± 60.9 μm and mean tensile strength was equal to 375.1 ± 248.3 MPa. For the purpose of this work, the fibers were cut to a length of 2–3 mm.

Composite fabrication

PLA pellets and fibers were dried in a vacuum oven at 98°C for 3 h. PLA composites were manufactured using a twin-screw microextruder (DSM Explore 5&15 CC Micro Compounder) and mixing process

parameters (50 rpm screw speed, 1-min mixing time, and temperature profile: 165–185–200°C) were modulated to optimize material final properties. To obtain the desired specimens for the characterization, the molten composite samples were transferred after extrusion through a preheated cylinder to a mini injection ($T_{\text{mold}} = 25^{\circ}\text{C}$, $P_{\text{injection}} = 8$ bar). Composites were prepared with different amount of phormium fibers: specifically, a master batch containing 40 wt % of phormium fibers was prepared (PLA40PH), whereas the other compositions (20 and 30 wt % (designed as PLA20PH and PLA30PH, respectively) were obtained diluting the master with neat PLA.

Thermal analysis of PLA/phormium composites

Thermogravimetric analysis (TGA) was performed on 10 mg samples on a Seiko Exstar 6000 TGA quartz rod microbalance. The tests were carried out in nitrogen flow (250 mL/min) from 30 to 900°C with a 10°C/min heating ramp.

The melting and crystallization behavior of the matrix polymer and the composites were studied using a differential scanning calorimeter (DSC, Mettler Toledo 822/e Model), calibrated with an indium sample. Ten milligrams of dried samples were placed in covered aluminum sample pans and then placed in the DSC sample holder. The samples were first heated at 10°C/min in the –25 to 250°C temperature range in nitrogen atmosphere (to eliminate the thermal history of the sample), then cooled at the same rate from 250 to –25°C and heated again. Melting and cold crystallization temperatures and enthalpies (T_m , T_{cc} and ΔH_m , ΔH_{cc}) were determined from the first and the second heating scan, while glass transition temperature (T_g) was measured from the heating and cooling scans. The crystallinity degree of the samples was calculated taking as reference 94 J/g as heat of melting of the fully crystalline sample¹⁸ according to the following eq. (1)⁸:

$$X_c = \frac{(\Delta H_m - \Delta H_{cc})}{\Delta H_{m0}(1 - w_f)} \quad (1)$$

where ΔH_m is the melting enthalpy, ΔH_{cc} is the enthalpy of cold crystallization, ΔH_{m0} is enthalpy of melting for a 100% crystalline PLA sample, and $(1 - w_f)$ is the weight fraction of PLA in the sample.

FTIR analysis

IR spectra of the materials were recorded using a Jasco FTIR 615 spectrometer in the frequency range 4000–500 cm⁻¹, operating in attenuated total reflectance (ATR) mode.

Scanning electron microscopy

A Hitachi S-2500 scanning electron microscope was used to investigate fracture surfaces of composites. Prior to observation, the specimens were graphite coated.

Disintegrability in composting

Disintegration patterns of PLA and PLA-phormium fiber composites were observed through a disintegration test in composting conditions according to the ISO 20200 standard, which defines disintegrated a sample that achieves in 90 days the 90% of disintegration, namely, after this period, 10% only has to be retained in a 2-mm sieve. Samples of dimensions $5 \times 5 \times 2 \text{ mm}^3$ were buried into an organic substrate and incubated at 58°C . The test is supposed to simulate a real composting process. A specific quantity of compost, supplied by Gesenu S.p.a., was mixed together with the synthetic biowaste, prepared with certain amount of sawdust, rabbit food, starch, sugar, oil, and urea. The water content of the substrate was around 50 wt % and the aerobic conditions were guaranteed by mixing it softly. Samples were then buried at 4–6 cm depth in perforated boxes, containing the prepared mix, and incubated at 58°C . The samples were recovered at different disintegration steps and washed with distilled water, dried in oven at 37°C for 24 h, and weighted with an analytical balance. Microstructure of PLA and PLA composites at 10, 20, 30, and 40 days of incubation in composting was investigated by scanning electronic microscopy. Photographs of the samples were taken for visual comparison. Also in this case, DSC (Mettler Toledo 822/e) measurements were performed in the temperature range from -25 to 250°C , at $10^\circ\text{C}/\text{min}$, performing two heating and one cooling scans. TGA (Seiko Exstar 6000) was performed on 10-mg weight samples, in nitrogen flow (250 mL/min), from 30 to 900°C at $10^\circ\text{C}/\text{min}$ heating rate. Fourier infrared spectra of the samples in the $400\text{--}4000 \text{ cm}^{-1}$ range were recorded by a Jasco FTIR 615 spectrometer in ATR mode.

RESULTS

Thermal properties of PLA/phormium composites

Figure 1 shows the DSC thermograms obtained from the first and second heating scan of PLA and phormium-based composites at time 0 (before disintegration test). The structure is obviously modified after the first scanning is performed, but to compare two materials with different thermal history it is important to eliminate the processing history, which is the reason why a second heating scan is considered more reliable. The samples displayed on heating

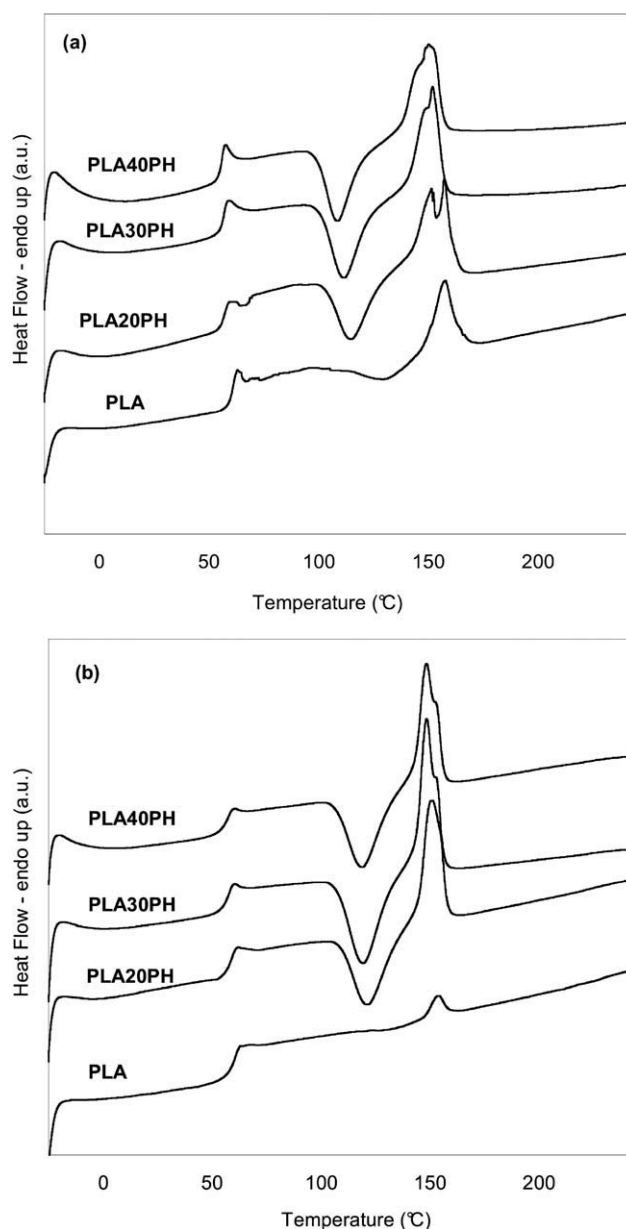


Figure 1 Heat flow for the first (a) and second (b) heating cycles obtained from the DSC for neat PLA and PLA-based composites before disintegration tests.

three main transitions: a glass transition (T_g), a cold crystallization exotherm (T_{cc}), and a melting endotherm (T_m). The crystallinity values, such as crystallization enthalpy (ΔH_{cc}) and melting enthalpy (ΔH_m) for samples before disintegration tests, are reported in Table I. From DSC analysis, the PLA appears to be practically amorphous, which is not surprising, because a polymer with slow nucleation and crystallization rates has been used.⁸ Moreover, the T_g of the PLA/phormium composites appeared slightly affected by the composition, with a moderate decrease with increasing phormium content. The introduction of fibers did not result in a significant variation in the position of the peaks, except for the

TABLE I
Enthalpies and Crystallinity Degree (X_c) Referred to the Second Heating Cycle for PLA/Phormium Composites Before Disintegration Tests

Materials	ΔH_{cc} (J/g)	ΔH_m (J/g)	X_c (%)
PLA	1.7 ± 0.3	2.7 ± 0.1	1.02 ± 0.32
PLA20PH	21.9 ± 1.5	23 ± 1.0	1.41 ± 0.70
PLA30PH	21.8 ± 1.0	22.8 ± 0.2	1.46 ± 1.30
PLA40PH	18.7 ± 1.2	19.4 ± 0.9	1.21 ± 0.56

melting peak,¹⁹ which appears lower by $\sim 5\text{--}7^\circ\text{C}$ for the composites with respect to the pure matrix. A decrease of melting enthalpy and cold crystallization enthalpy with growing fiber content is also measured.²⁰ The cold crystallization peak was shifted to lower temperatures with the addition of phormium fibers with respect to neat PLA. This is in agreement with findings from literature²¹ indicating that the presence of fillers can promote the cold crystallization of PLA matrix. A slight increase in crystallinity was also measured, due to the nucleating effect of fibers. The double melting peak visible in DSC thermograms was attributed to a lamellar rearrangement during crystallization, as observed also in previous works on PLA/hemp and wood composites.²²

The thermal stability of neat PLA and PLA based composites was investigated in terms of weight loss as a function of temperature by TGA. In Figure 2, differential residual mass (DTG) is reported for PLA and PLA/phormium composites before the disintegration tests. As it has been reported elsewhere for kenaf and PLA,²³ also in the case of phormium fibers, the degradation temperatures of the fiber and matrix are comparable. The thermal degradation of phormium fibers occurs in two main stage process,²⁴

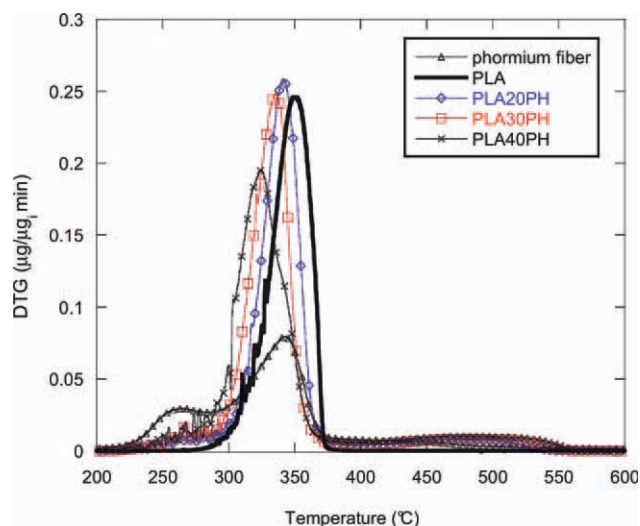


Figure 2 Differential residual mass obtained from the TGA analysis for neat phormium fiber, PLA, and PLA-phormium composites. [Color figure can be viewed in the online issue, which is available at wileyonlinelibrary.com.]

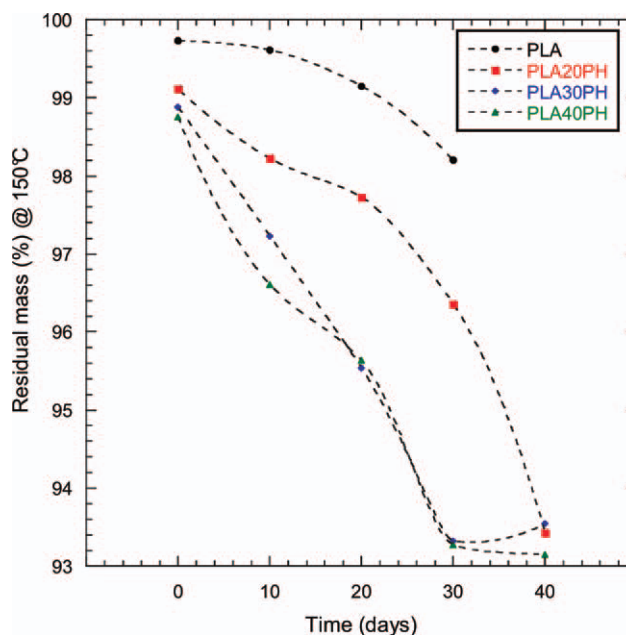


Figure 3 Residual mass at 150°C for PLA and PLA-phormium composites. [Color figure can be viewed in the online issue, which is available at wileyonlinelibrary.com.]

where most cellulose decomposition occurs at temperature of 337°C . The main degradation peak for PLA was shifted to lower temperatures for all PLA/phormium composites, decreasing the thermal stability of the different systems.²⁵ To offer more indications on disintegration, the residual mass at 150°C for PLA and PLA-phormium composites was reported in Figure 3. The weight loss is very close to zero in all cases, although for longer exposure to the compost some limited moisture absorption from the residue of the fibers was measured.

Disintegrability in composting of PLA/phormium composites

Disintegrability in composting conditions was first evaluated by visual observation of the PLA and PLA composites. The effects of gradual decomposition of PLA and PLA/phormium composites with different fiber volumes during their soil burial test for times up to 40 days are depicted in Figure 4. Here, the progressive darkening of the samples is clearly observed: in particular, PLA sample is increasingly opaque. The color changes could be a signal that the hydrolytic degradation process of the polymer matrix has started, thus inducing a change in the refraction index of the sample as the consequence of water absorption and/or presence of products formed by the hydrolytic process.²⁶ In this case, the color changes are also linked with sample degradation process and embrittlement, leading to their breakage, and especially to the progressive evidence of

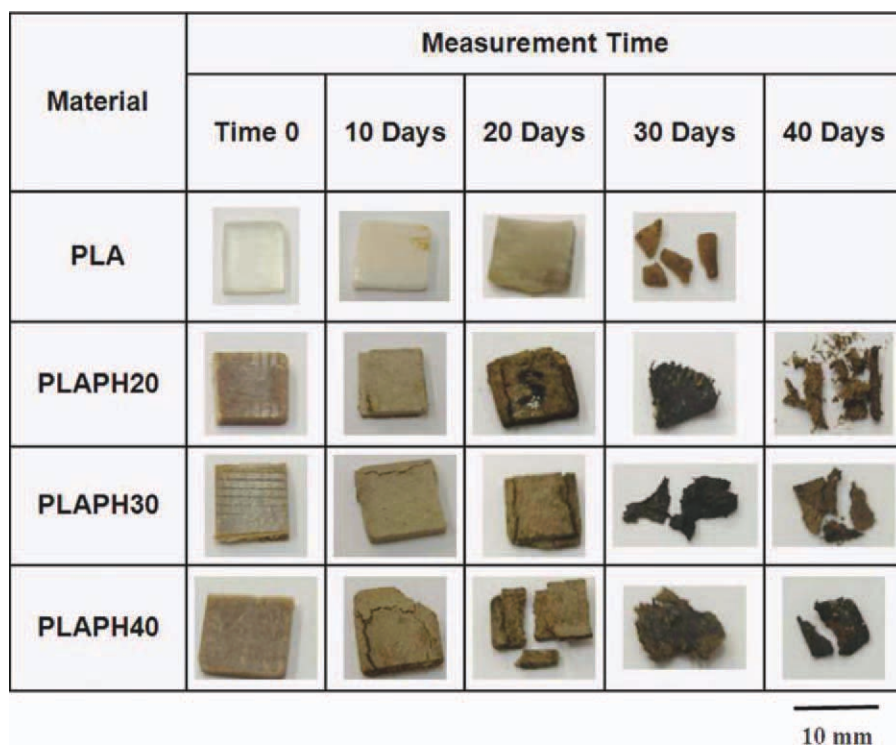


Figure 4 Photographs of neat PLA and PLA/phormium composites at different incubation times. [Color figure can be viewed in the online issue, which is available at wileyonlinelibrary.com.]

phormium fibers, which are darker in color than PLA, over the bulk of the composite.

PLA matrix at 40 days is virtually disappeared, which implies that after this time only phormium fibers are remaining in the composite samples: the time for the disappearance of PLA is thus slightly lower than that revealed, e.g., in Ref. 27. This was explained with the fact that the PLA used in the present work has a very low crystallinity.

The disintegrability in composting conditions was evaluated in terms of mass loss at different incubation times. The disintegration process takes place between 20 and 30 days of incubation, as reported in Figure 5. The disintegrability value remains constant for all systems until 10 days of incubation, while reaches 15–20% at 20 days and then 60% at 30 days for all PLA based systems. Moreover, all the composites under study show the same kinetic of degradation at different times. The final amount of fibers after 40 days is lower than the initial value introduced in the composites (e.g., from the PLA20PH composite <20% in weight is remaining after dissolution of PLA); this suggests that the fibers degrade as well during the process, probably because of removal of nonstructural matter. To clarify which was the chemical environment to which the samples are exposed, compost was left to settle for some further time after the final measurements: it came out that the pH value after 60 days of maturation was equal to 7.98.

Figure 6 shows the DSC thermograms obtained from the first and second heating cycles. The glass transition temperature (T_g), crystallization temperature (T_{cc}), melting temperatures (T_{m1} and T_{m2}), obtained from analysis of DSC studies at different

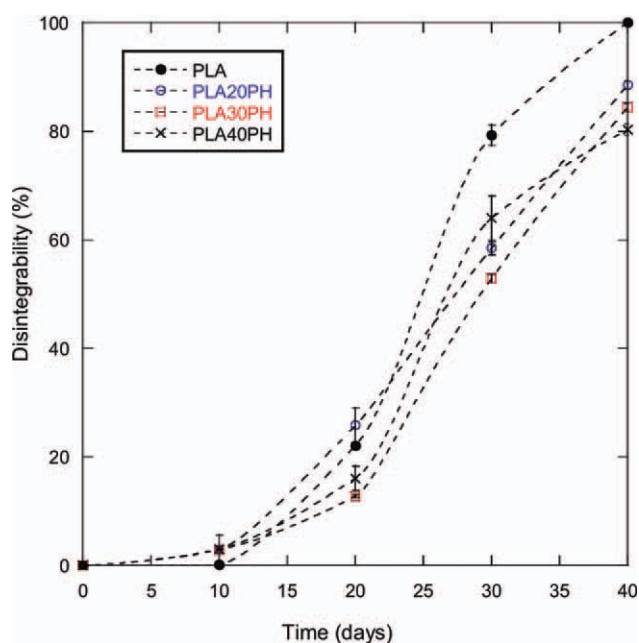


Figure 5 Disintegration curves of neat PLA and PLA/phormium composites. [Color figure can be viewed in the online issue, which is available at wileyonlinelibrary.com.]

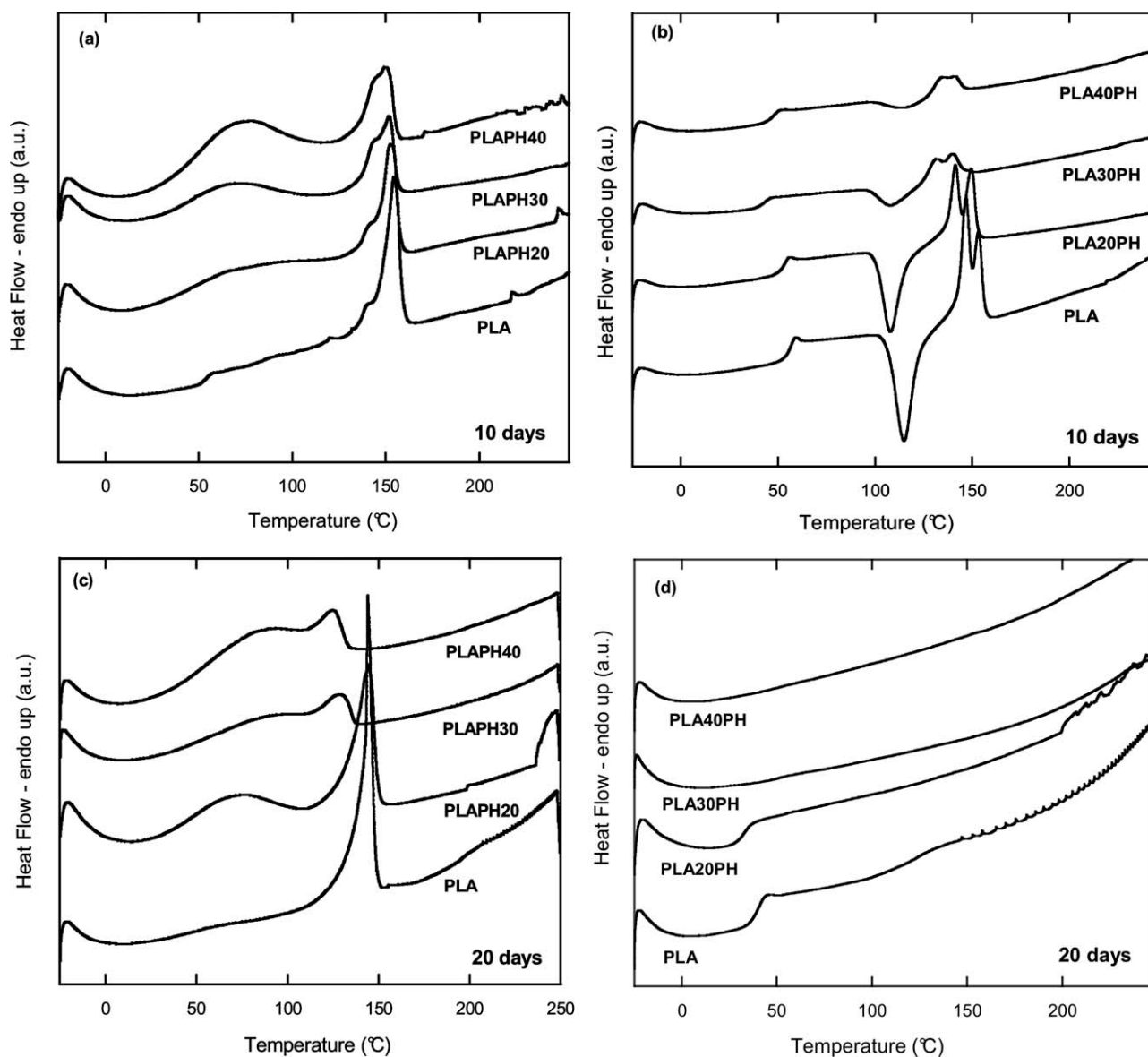


Figure 6 DSC curves for neat PLA and phormium composites at 10 days [(a) first scan and (b) second scan] and 20 days [(c) first scan and (d) second scan] incubation time.

TABLE II
Glass Transition Temperature (T_g), Cold Crystallization Peak (T_{cc}), and Melting Peaks (T_{m1} , T_{m2}), Referred to the Second Heating Cycle, for Neat PLA (a) and Phormium-Based PLA Composites at Different Stages of Disintegration

	T_g (°C)	T_{cc} (°C)	T_{m1} (°C)	T_{m2} (°C)	T_g (°C)	T_{cc} (°C)	T_{m1} (°C)	T_{m2} (°C)
	PLA				PLA20PH			
0 days	60.7 ± 0.6	132.2 ± 1.3	153.3 ± 0.3	–	59.2 ± 1.9	119.8 ± 1.9	150.9 ± 2.7	–
10 days	55.5 ± 1.5	115.1 ± 0.9	146.8 ± 0.4	153.6 ± 0.5	53.4 ± 1.3	107.9 ± 1.0	141.8 ± 1.9	145.0 ± 1.5
20 days	39.4 ± 3.3	–	–	–	32.1 ± 2.4	–	–	–
30 days	49.8 ± 1.4	–	–	–	47.9 ± 3.3	–	–	–
40 days	–	–	–	–	–	–	–	–
	PLA30PH				PLA40PH			
0 days	57.8 ± 0.2	119.2 ± 0.4	148.4 ± 0.1	152.7 ± 0.4	57.7 ± 0.4	118.2 ± 0.8	148.2 ± 1.9	153.1 ± 1.8
10 days	47.1 ± 1.3	108.0 ± 2.3	134.4 ± 4.7	142.9 ± 4.2	48.2 ± 0.8	114.9 ± 1.3	134.9 ± 0.9	142.1 ± 0.9
20 days	50.4 ± 1.7	–	–	–	48.9 ± 4.0	–	–	–
30 days	–	–	–	–	–	–	–	–
40 days	–	–	–	–	–	–	–	–

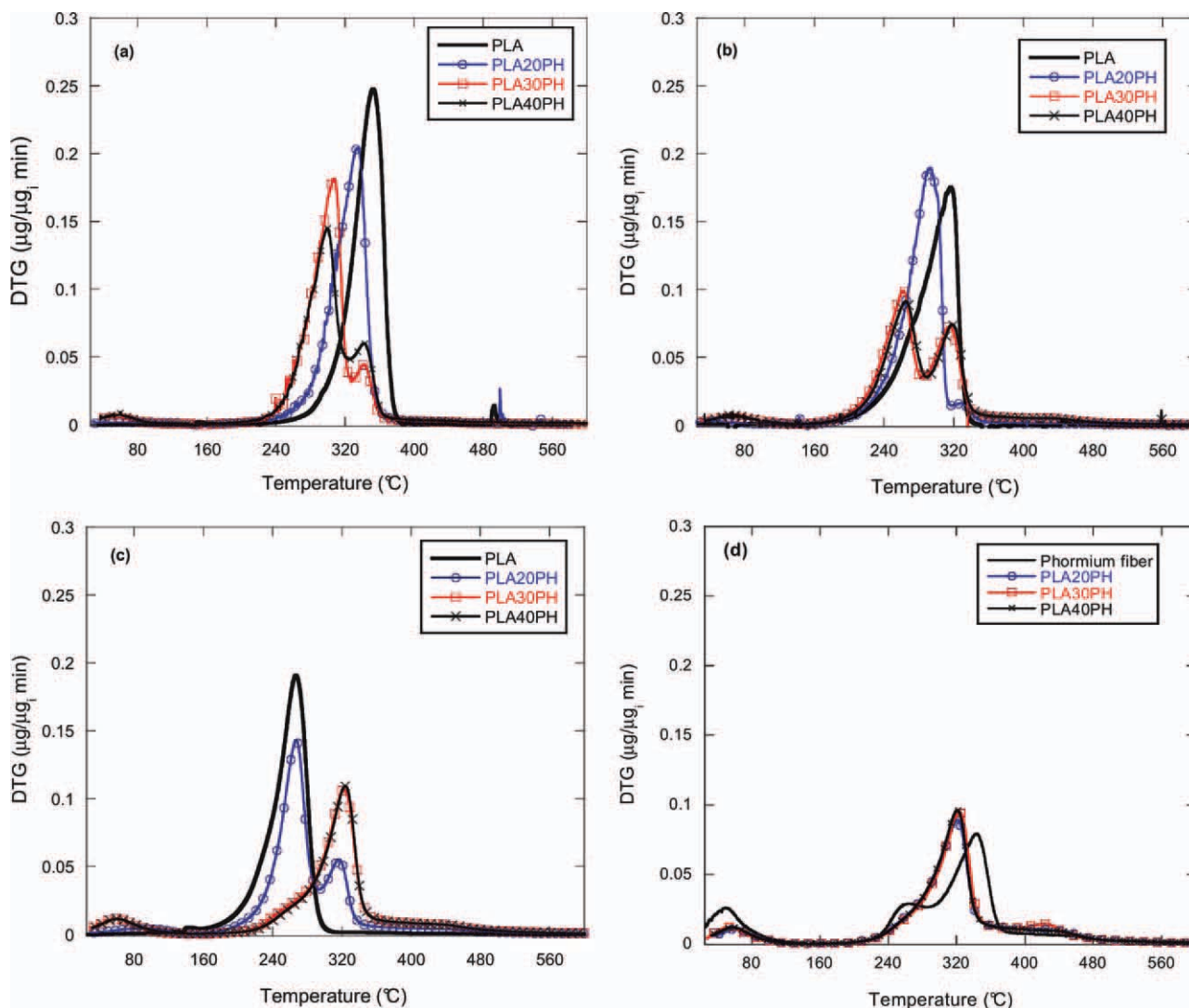


Figure 7 Weight loss rate for neat PLA and phormium composites at 10 days (a), 20 days (b), 30 days (c), and 40 days (d) incubation time. [Color figure can be viewed in the online issue, which is available at wileyonlinelibrary.com.]

incubation times, are summarized in Table II. The results are obtained from a series of at least three scans. The peak due to the glass transition temperature appears at a gradually lower temperature during biodegradation due to moisture absorption and gradually disappears in composites with increasing amounts of phormium fibers. Moreover, the gradual disintegration of PLA does not allow the observation of cold crystallization and melting peaks at composting times above 10 days. The double peak observable in correspondence with melting temperature is being related to the presence of two crystalline phases.²⁸ This is increasingly visible with higher fiber content, a fact suggesting that phormium fibers are able to favor the formation of the secondary crystalline phase, as happens in other cases of introduction of vegetable products in biopolymers.²⁹

TGA confirms this result and more details are shown in Figure 7. A slight weight loss around 70°C

is always apparent, due to moisture absorption in the compost. To better clarify this point, the water loss between 30 and 150°C as measured both from TGA and DSC tests, as shown in Tables III and IV, respectively. The agreement, in terms of water contents calculated from both techniques, confirmed that, as expected, higher water contents are revealed with increasing value of incubation time and

TABLE III
Water Loss (%) Between 30 and 150°C, as Measured From TGA

Materials	Water loss (%) 30–450°C from TGA				
	Time 0	10 days	20 days	30 days	40 days
PLA	0.27	0.39	0.85	1.80	0
PLA20PH	0.89	1.77	2.27	3.64	6.57
PLA30PH	1.12	2.77	4.46	6.68	6.46
PLA40PH	1.25	3.39	4.36	6.73	6.85

TABLE IV
Water Loss (%) Between 30 and 150°C, as Measured from DSC

Materials	Water loss (%) 30–450°C from DSC				
	Time 0	10 days	20 days	30 days	40 days
PLA	–	–	–	–	–
PLA20PH	–	0.83 ± 0.01	1.18 ± 0.08	0.62 ± 0.31	2.91
PLA30PH	–	1.43 ± 0.22	0.73 ± 0.15	5.45 ± 0.67	7.55
PLA40PH	–	2.12 ± 0.27	1.14 ± 0.35	5.77 ± 0.83	6.75

TABLE V
Peak Temperatures from DTG Data

Materials	T_{peak} (°C)				
	0 days	10 days	20 days	30 days	40 days
PLA	350	352.5	316.4	266.7	–
PLA20PH	341.1	335	292.4	267.7	–
	–	–	327.1 ^a	316.7 ^a	319.2 ^a
PLA30PH	334.4	307.5	261.8	–	–
	–	342.2 ^a	317.8 ^a	321 ^a	319.2 ^a
PLA40PH	322.7	299.2	265.8	–	–
	342.6 ^a	341.7 ^a	318.2 ^a	325 ^a	319.2 ^a

^a Peak related to fiber degradation.

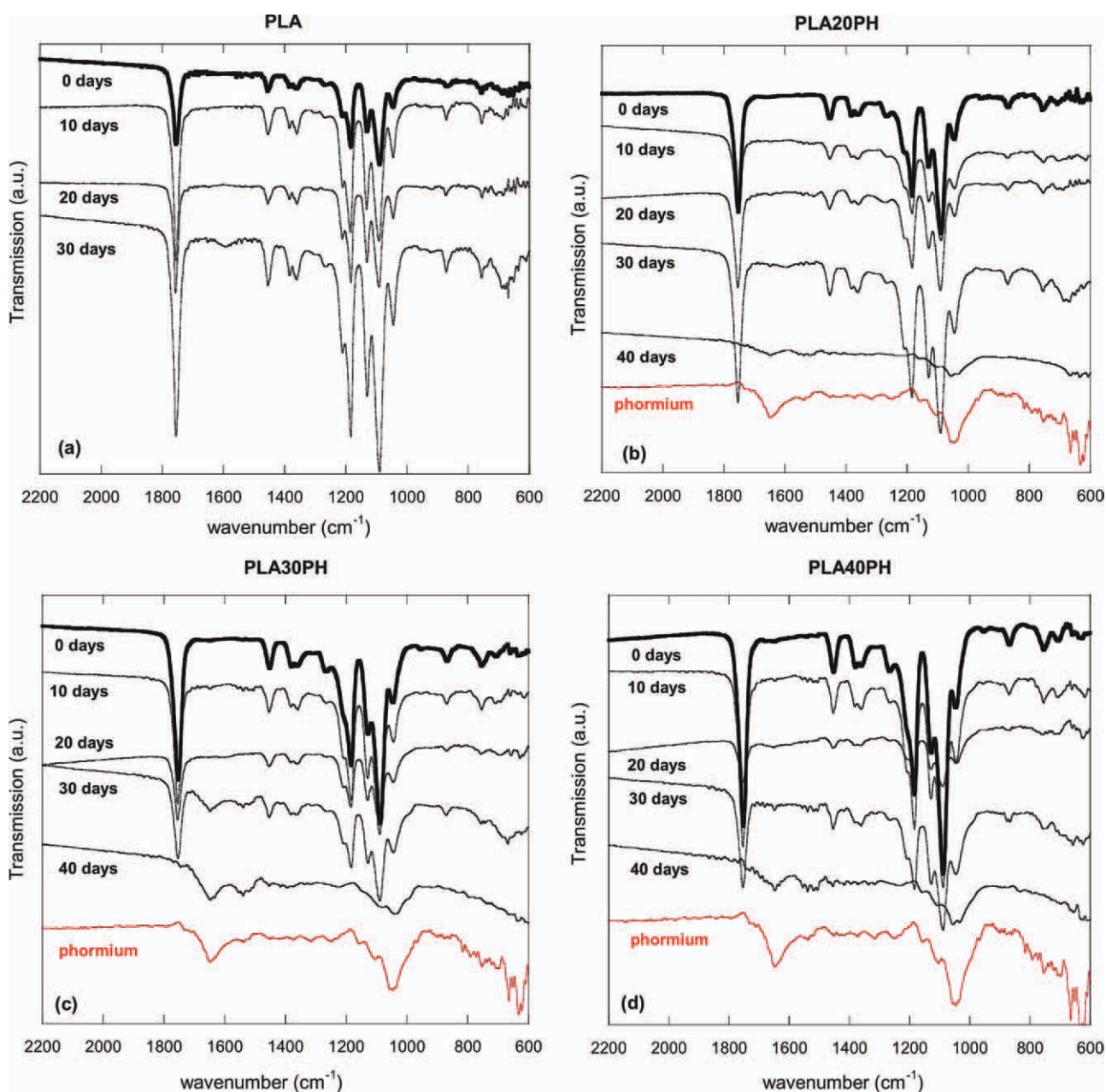


Figure 8 ATR spectra for (a) neat PLA, (b) PLA20PH, (c) PLA30PH, and (d) PLA40PH at different incubation times. [Color figure can be viewed in the online issue, which is available at wileyonlinelibrary.com.]

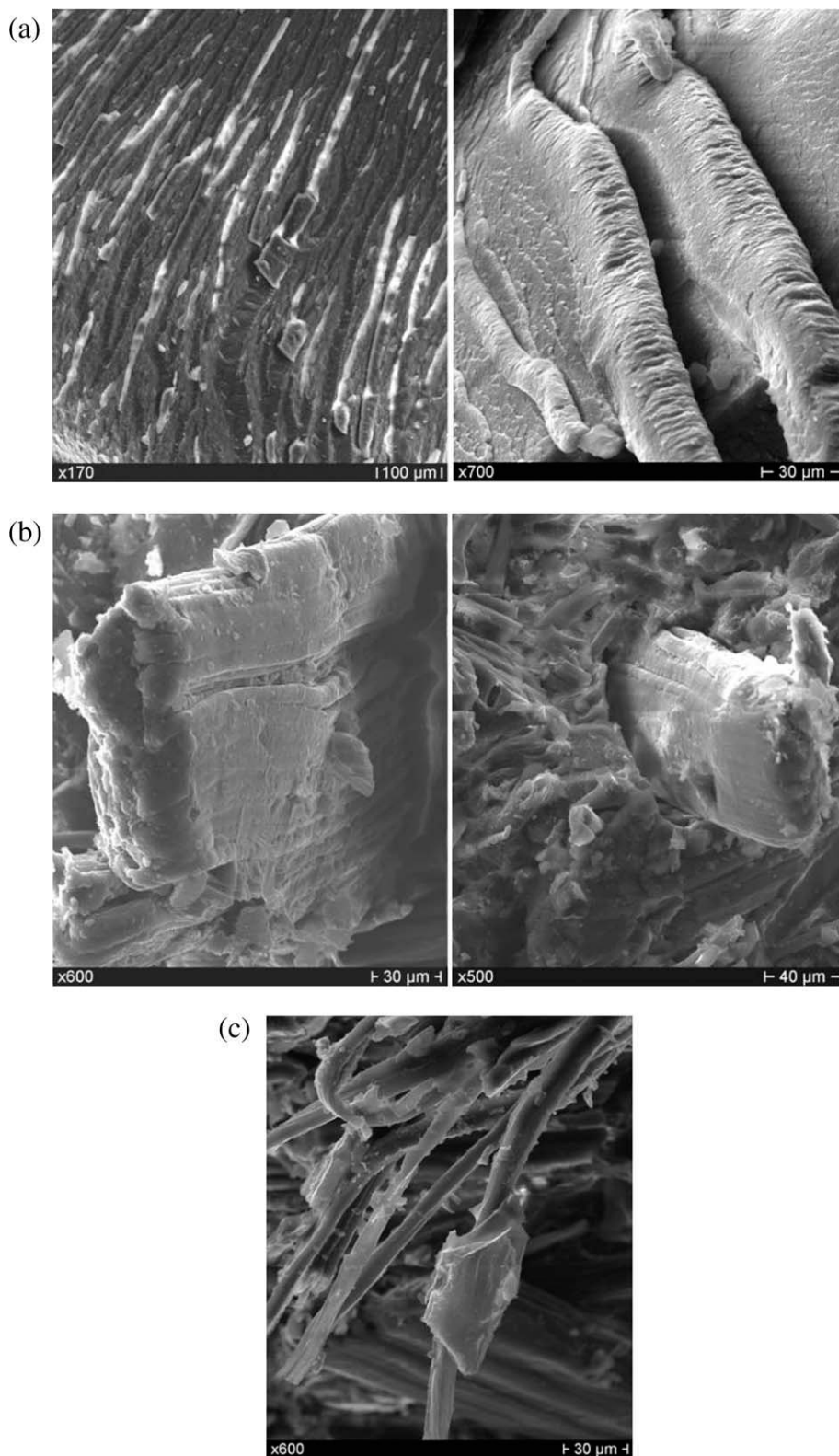


Figure 9 (a) PLA (10 days) showing erosion grooves. (b) PLA30PH (10 days) (left) and PLA40PH (10 days) (right) showing fragmentation patterns of PLA around phormium fibers. (c) PLA 30PH (10 days) (left) and PLA40PH (10 days) (right) showing fiber-matrix de-adhesion.

phormium fibers. Moreover, Figure 7 highlights that two main peaks are visible between 250 and 350°C, one associated with degradation of PLA and the

other associated with degradation of phormium fibers, the latter being at higher temperature than the former. The peak temperatures values are

reported in Table V. The peak associated to phormium fibers becomes clearly visible after 10 days for both PLAPH30 and PLAPH40, and it appears at 20 days also for PLAPH20. After 30 days, the peak associated to fibers is more evident than the one associated to the matrix. Finally, at 40 days, in all composites only the phormium fiber peak is visible, confirming the total disintegration of PLA, as found in soil burial experiments. It is suggested that the peak temperature for DTG associated to the matrix is decreased by the growing presence of phormium fibers. The analysis of the residual mass at 400°C confirmed that neat PLA is completely disappeared at this temperature, while the composites are reduced to less than 0.01% of the initial weight.

Figure 8 shows the FTIR spectrum of the samples at different incubation times. The infrared spectra of PLA composites display the typical stretching of carbonyl group (—C=O) at 1750 cm^{-1} by lactide, and the —C—O— bond stretching in the —CH—O— group of PLA at 1182 cm^{-1} . The intensities of the —C=O bands of PLA show sharpening and increase after biodegradation. The changes of —C=O band are associated with the increase in the number of carboxylic end groups in the polymer chain during the hydrolytic degradation.³⁰ The FTIR spectrum of phormium fiber is shown at the bottom of the figures for comparison: this shows clearly OH bending due to absorbed water (around 1560 cm^{-1}) and a second large peak in the region between 1100 and 1050 cm^{-1} , which is generally the band region for ring stretching, C—C and —C—O stretching and C—H bending.³¹ These structural movements are likely to take place in cellulose but also possibly in hemicellulose or lignin, which are both known to be well present in phormium fibers: the peak between 1100 and 1050 cm^{-1} was also noted in Ref. 17, although the authors did not comment about it.

Morphological characterization of PLA/phormium systems after different incubation times was carried out to evaluate the effect of composting conditions on the composite structure. Scanning electron micrographs (Fig. 9) show PLA surface as characterized by regular transverse striations after some time of degradation. These could be generated by the accumulated erosion of the amorphous macromolecules on the surface, giving rise to the deeper grooves [Fig. 9(a)]. This is quite typical in cases where PLA has not a very high crystallinity, and it is subjected to soil burial, which implies the exposure to a non-neutral environment.^{32,33} However, it is confirmed also in this case, where used compost has an only slightly basic pH, as mentioned above. The presence of the fibers gives rise to an accentuate breakage of PLA, resulting in progressive fragmentation growing for higher fiber content, as depicted in Figure 9(b). This results in increasing de-adhesion of fibers, as

indicated in Figure 9(c), where it is also clear as adequate impregnation is no longer provided on the bulk of the fibers, which appear in some places deprived from resin.

As a general consideration, the disintegration process is triggered by two main factors, which are the low crystallinity of the PLA matrix used and the percent of phormium fiber used in the composite: both are well known occurrences in biopolymers.³⁴ These factors would need to be accurately dealt with in selecting matrix and fiber content for possible applications of a fully biodegradable and compostable phormium-reinforced polymer composite.

CONCLUSIONS

This work on the disintegration patterns of composites obtained introducing *Phormium tenax* fibers in a PLA matrix gives promising results for the applicability of these composites, even in a context where fast disintegration, leading to compostability is required. For this purpose, a low-crystallinity PLA has been used, which shows an early onset of disintegration by deep erosion of the surface, leading in composites to fiber-matrix debonding. In addition, the peak temperature for degradation of PLA is decreased by the growing presence of phormium fibers.

In general, the results appear promising for a possible use of these composites, whenever a rapid disintegration leading to easy compostability of the material is required, the results being comparable to what obtained with other PLA-based composites reinforced with other plant fibers (e.g., kenaf).

The authors acknowledge Gesenu S.p.a. for compost supply, which was necessary to obtain synthetic biowaste.

References

1. Serizawa, S.; Inoue, K.; Iji, M. *J Appl Polym Sci* 2006, 100, 618.
2. Oksman, K.; Skrifvars, M.; Selin, J. F. *Compos Sci Technol* 2003, 63, 1317.
3. Liu, L.; Li, S.; Garreau, H.; Vert, M. *Biomacromolecules* 2000, 1, 350.
4. Fambri, L.; Migliaresi, C. In *Poly(lactic acid): Synthesis, Structures, Properties, Processing, and Applications*; Auras, R.; Lim, L.-T.; Selke, S. E. M.; Tsuji, H., Eds.; Wiley: Hoboken, NJ, 2010; Chapter 9, pp 113–124.
5. Fukushima, K.; Abbate, C.; Tabuani, D.; Gennari, M.; Camino, G. *Polym Degrad Stab* 2009, 94, 1646.
6. Tsuji, H.; Mizuno, A.; Ikada, Y. *J Appl Polym Sci* 1998, 70, 2259.
7. Mukherjee, T.; Kao, N. *J Polym Environ* 2011, 19, 714.
8. Fortunati, E.; Armentano, I.; Iannoni, A.; Kenny, J. M. *Polym Degrad Stab* 2010, 95, 2200.
9. Liu, L.; Fishman, M. L.; Hicks, K. B.; Liu, C. K. *J Agric Food Chem* 2005, 53, 2017.
10. Wehi, P. M.; Clarkson, B. D. *NZ J Botany* 2007, 45, 521.
11. LeGuen, M. J.; Newman, R. H. *Compos Part A* 2007, 38, 2109.

12. Newman, R. H.; Clauss, E.; Carpenter, J.; Thumm, A. *Compos Part A* 2007, 38, 2164.
13. Newman, R. H.; Le Guen, M. J.; Battley, M. A.; Carpenter, J. E. P. *Compos Part A* 2010, 41, 353.
14. De Rosa, I. M.; Santulli, C.; Sarasini, F. *Mater Des* 2010, 31, 2397.
15. De Rosa, I. M.; Iannoni, A.; Kenny, J. M.; Puglia, D.; Santulli, C.; Sarasini, F.; Terenzi, A. *Polym Compos* 2011, 32, 1362.
16. Modi, S. J. Assessing the Feasibility of Poly-(3-hydroxybutyrate-co-3-hydroxyvalerate) (PHBV) and Poly-(lactic acid) for Potential Food Packaging Applications. Thesis, Graduate Program in Food Science and Nutrition, The Ohio State University, 2010.
17. Duchemin, B.; Staiger, M. P. *J Appl Polym Sci* 2009, 112, 2710.
18. De Rosa, I. M.; Kenny, J. M.; Puglia, D.; Santulli, C.; Sarasini, F. *J Reinf Plast Compos* 2010, 29, 3450.
19. Huda, M. S.; Drzal, L. T.; Misra, M.; Mohanty, A. K. *J Appl Polym Sci* 2006, 102, 4856.
20. Wielage, B.; Lampke, T.; Marx, G.; Nestler, K.; Starke, D. *Thermochim Acta* 1999, 337, 169.
21. Wu, D.; Wu, L.; Xu, B.; Zhang, Y.; Zhang, M. *J Polym Sci Part B* 2007, 45, 1100.
22. Islam, M. S.; Pickering, K. L.; Foreman, N. J. *Compos Part A* 2010, 41, 596.
23. Colom, X.; Carrasco, F.; Pagès, P.; Cañavate J. *Compos Sci Technol* 2003, 63, 161.
24. Avella, M.; Bogoeva-Gaceva, G.; Bužarovska, A.; Errico, M. E.; Gentile, G.; Grozdanov, A. *J Appl Polym Sci* 2008, 108, 3542.
25. Krause Sammartino, L. M.; Aranguren, M. I.; Reboredo, M. M. *J Appl Polym Sci* 2010, 115, 2236.
26. Li, S.; Girard, A.; Garreau, H.; Vert, M. *Polym Degrad Stab* 2001, 71, 61.
27. Li, S.; McCarthy, S. *Biomaterials* 1999, 20, 35.
28. Fukushima, K.; Tabuani, D.; Abbate, C.; Arena, M.; Ferreri, L. *Polym Degrad Stab* 2010, 95, 2049.
29. Sandeep, S. A.; Mohanty, A. K.; Misra, M. *Compos Sci Technol* 2011, 71, 653.
30. Kumar, R.; Yakubu, M. K.; Anandjiwala, R. D. *Exp Polym Lett* 2010, 4, 423.
31. Hinterstoisser, B.; Akerholm, M.; Salmen, L. *Carbohydr Res* 2001, 334, 27.
32. Gijpferich, A. *Biomater* 1996, 17, 103.
33. Yuana, X.; Mak, A. F. T.; Yao, K. *Polym Degrad Stab* 2003, 79, 45.
34. Yussuf, A. A.; Massoumi, I.; Hassan, A. *J Polym Environ* 2010, 18, 422.